Acta Cryst. (1994). D**50**, 167-174

Structure of [2Fe-2S] Ferredoxin I from *Equisetum arvense* at 1.8 Å Resolution

BY SHINJI IKEMIZU

The Graduate University for Advanced Studies, Oho, Tsukuba, Ibaraki 305, *Japan*

MASAHIKO BANDO, TAKAO SATO, YUKIO MORIMOTO AND TOMITAKE TSUKIHARA*

Department of Biological Science and Technology, Faculty of Engineering, The University of Tokushima, Tokushima 770, *Japan*

AND KEIICHI FUKUYAMA

Department of Biology, Faculty of Science, Osaka University, Toyonaka, Osaka 560, *Japan*

(*Received* 14 *June* 1993; *accepted* 13 *September* 1993)

Abstract

Ferredoxin I (Fd I) from *Equisetum arvense* is an iron-sulfur protein composed of 95 amino-acid residues and one [2Fe-2S] cluster. It crystallized in the space group $P2_1$, a = 30.4, b = 57.4, c = 47.5 Å and β = 78.7° with two molecules per asymmetric unit. X-ray diffraction data up to 1.8 Å resolution were collected by using a Rigaku four-circle diffractometer. The initial model of Fd I, which was derived by the molecular replacement method using a structure of the Fd I from the blue-green alga *Aphanothece sacrum*, was refined by molecular dynamics simulation and a least-squares minimization with stereochemical restraints. Positional parameters and isotropic temperature factors for 1420 non-H protein atoms and 183 water molecules were refined on 13 838 observed structure factors ($F_o > \sigma_{Fo}$) between 10.0 and 1.8 Å resolution. The final R factor was 17.0%, and the standard deviation of atomic position estimated by Luzzati plot [Luzzati (1952). *Acta Cryst.* **5**, 802-810] was 0.2 Å. The electron-density map was well defined for the two independent molecules except for the N-terminal residue and the three C-terminal residues. Equivalent Cα atoms of two independent molecules in the asymmetric unit were superposed by the least-squares method with root-mean-square deviations of 0.26 Å. Reasonable structural differences were observed at a polypeptide segment having few intramolecular interactions. Highly flexible regions of the molecule were assigned from the structural differences between the two independent molecules in the crystal and the distribution of temperature factors along the polypeptide chain.

Introduction

Plant-type ferredoxins (Fd's) function as redox components in photosynthetic system I and other metabolic systems with low redox potentials at about -400 mV (Lovenberg, 1973, 1977). They have been isolated from a wide range of plants and algae, and contain two Fe and two inorganic S atoms, [2Fe-2S] (Matsubara & Saeki, 1992). They are composed of 93-99 amino-acid residues; the amino-acid sequences of typical plant-type Fd's (Matsubara & Hase, 1983) are given in Fig. 1. The sequences are apparently homologous to each other. The crystal structures of [2Fe-2S] ferredoxins from *Spirulina platensis* (Fukuyama *et al.*, 1980; Tsukihara *et al.*, 1981), *Aphanothece sacrum* (Tsukihara *et al.*, 1990) and anabaena 7120 (Rypniewski *et al.*, 1991) were solved at 2.5, 2.2 and 2.5 Å resolution, respectively. These three Fd's exhibit essentially the same polypeptide-chain folding. Similar folding motifs were found in ubiquitin (Vijay-Kumar, Bugg & Cook, 1987) and the IgG-binding domain of protein G (Gronenborn *et al.*, 1991), both of which are functionally distinct and unrelated in sequence to Fd's.

The [2Fe-2S] Fd I from *Equisetum arvense* consists of 95 amino-acid residues (Hase, Wada & Matsubara, 1977) and has a relative molecular mass of 10 263. The amino-acid sequence of this protein differs from that of the *A. sacrum* Fd I by 58%. Although the three-dimensional structures for the three Fd's are known at medium resolution, a detailed structure is required for the design of a protein-engineering protocol (Hase, personal communication) and for correlation with the results of spectroscopic studies (Mino, Loehr, Wada, Matsubara & Sanders-Loehr, 1987; Dugad, LaMar, Banci & Bertini, 1990; Oh & Markley, 1990). The crystals of *E. arvense* Fd I diffract to at least 1.8 Å resolution and are suitable for high-resolution X-ray analysis. As an asymmetric unit of the crystal consists of two molecules, the structures of these molecules were compared to discover any structural flexibility in [2Fe-2S] Fd's. Here we report the crystal structure of *E. arvense* Fd I at 1.8 Å resolution, which is the most extensively refined [2Fe-2S] Fd structure.

* Author to whom correspondence should be addressed.

Crystallization and X-ray experiments

The [2Fe-2S] Fd of *E. arvense* was crystallized by the microdialysis technique. A protein solution comprising 1.0-2.0% Fd and 0.35 *M* NaCl in 0.1 *M* Tris/HCl buffer (pH 7.5) was dialyzed against 70% saturated ammonium sulfate in the same buffer at 278 K. Crystals grew to the size of about 0.3 × 0.3 × 0.6 mm in about one month. The space group is $P2_1$ with cell dimensions a = 30.4, b = 57.4, c = 47.5 Å and β = 78.7°. Assuming that the asymmetric unit contains two molecules, the V_m is 1.98 $Å^3$ Da^{-1} (Matthews, 1968); the low value of V_m indicates tight packing of the protein molecules in the crystal.

Intensity data were collected at 281 K by the continuous ω-scanning method on a Rigaku four-circle diffractometer using Ni-filtered Cu $K\alpha$ radiation operated at 40 kV and 200 mA. Each crystal was mounted in a thin-wall capillary with the b axis parallel to the φ axis of the goniometer. Backgrounds were measured at each end of the scanning range for 1/5 to 1/4 of the total scanning period. The intensities were corrected for Lorentz and polarization factors. A set of intensity data for the strong reflections within 1.8 Å resolution was used to scale intensity data sets. Four crystals were used to collect a full data set to 1.8 Å. The degradation of the crystals as a result of radiation damage was monitored by measuring intensities of standard reflections every 200 reflections. Intensities of the first several hundred reflections in each data collection were remeasured at the end of experiment in order to estimate the resolution dependence of the damage. Correction for the radiation damage was made with regard to an exposure period and the diffraction angle. An absorption correction was made according to the method described by North, Phillips & Matthews (1968). The intensities were also corrected as a function of the χ value of the diffractometer to minimize the deviation of the averaged ratio of $F(hkl)/F(h\bar{k}l)$ in each subset from 1.0; for some data sets these values deviated significantly from 1.0 at high χ angle. A total of about 21 000 independent reflections with Bijvoet pairs were obtained by averaging equivalent F values with weights $1/(\sigma_F)^2$. Some statistics of the observed structure factors are given in Table 1.

Respective averaged structure amplitudes for reflections of $h + k = 2n$ and $h + k = 2n + 1$ are shown in Fig. 2. The intensities for $h + k = 2n$ are significantly greater than those for $h + k = 2n + 1$ at low resolution. This indicates that the two molecules in the asymmetric unit are related by pseudo-C face-centered symmetry.

Structure determination

Structural model at low resolution

A Bijvoet difference Patterson function was calculated with coefficients of $|F(hkl) - F(\bar{h}\bar{k}\bar{l})|^2$ at 5 Å resolution to determine positions of [2Fe-2S] centers in the unit cell. Two [2Fe-2S] centers in the asymmetric unit were located at (0.523, 0.0, 0.064) and (0.023, 0.5, 0.064), which were related to one another by the C face-centered symmetry. Fixing the active centers at the above positions, the model molecules whose main-chain structures were the same as that of *A. sacrum* Fd (Tsukihara *et al.*, 1990) were rotated and the R factor, $R = \Sigma||F_o| - |F_c||/\Sigma|F_o|$, was calculated at each orientation. The resultant R-factor distribution gave 19 local minima. Out of 19 trial structures, nine were rejected because of overlap among molecules in the crystal.

For each of ten trial structures an anomalous-difference Fourier map was composed with coefficients of $[F(hkl) - F(\bar{h}\bar{k}\bar{l})]\exp(\alpha_c - \pi/2)$ at 5 Å resolution, where α_c is a phase angle from the atomic coordinates of the model. Only one of ten Fourier maps showed reasonable peaks at the expected sites for the [2Fe-2S] clusters. Consequently, a unique structural model was selected.

Structure refinement

In order to resolve the C face-centered symmetry of the model structure, two molecules with [2Fe-2S] centers at (0.523, 0.0, 0.064) and (0.023, 0.5, 0.064) were translated by (dx, dy, dz) and (-dx, -dy, -dz),

```
                                10                  20                  30                  40                  50
(1) E. arvense I        - A Y K T V L K T - P S G - E F T L D V P E G T T I L D A A E E A G Y D L P F S C R A G A C S S C L G K V
(2) E. arvense II       - A Y K V T L K T - P D G - D I T F D V E P G E R L I D I G S E K A - D L P L S C Q A G A C S T C L G K I
(3) A. sacrum I         A S Y K V T L K T - P D G - D N V I T V P D D E Y I L D V A E E E G L D L P Y S C R A G A C S T C A G K L
(4) S. oleraced         A A Y K V T L V T - P T G - N V E F Q C P D D V Y I L D A A E E E G I D L P Y S C R A G A C S S C A G K L
(5) P. americana II   A A S Y K V T F V T - P S G - T N T I T C P A D T Y V L D A A E E S G L D L P Y S C R A G A C S S C A G K V
(6) S. platensis         A T Y K V T L I N E A E G I N E T I D C D D D T Y I L D A A E E A G L D L P Y S C R A G A C S T C A G T I
                                10                  20                  30                  40                  50

                        51                  60                  70                  80                  90
(1) E. arvense I         V S G S V - D E S E G S F L D D G Q M E E G F V L T C I A I P E S D L V I E T H K E E E L F -
(2) E. arvense II        V S G T V - D Q S E G S F L D D E Q I E Q G Y V L T C I A I P E S D V V I E T H K E D E L - -
(3) A. sacrum I          V S G P A P D - E D Q S F L D D D Q I Q A G Y I L T C V A Y P T G D C V I E T H K E E A L Y -
(4) S. oleraced          K T G S L - N Q D D Q S F L D D D Q I Q A G Y I L T C A A Y P V S D V T I E T H K E E E L T A
(5) P. americana II      T A G A V - N Q E D G S F L E E E Q M E A G W V L T C V A Y P T S D V T I E T H K E E D L T A
(6) S. platensis         T S G T I - D Q S D Q S F L D D D Q I E A G Y V L T C V A Y P T S D C T I K T H Q E E G L Y -
                        54                  60                  70                  80                  90
```

Fig. 1. Amino-acid sequences of typical plant-type Fd's shown by single-letter notation. The upper numerals are sequence numbers for *E. arvense* Fd I, and the lower ones are common sequence numbers for the [2Fe-2S] Fd's. (1) *Equisetum arvense* I; (2) *Equisetum arvense* II; (3) *Aphanothece sacrum*; (4) *Spinacia oleracea*; (5) *Phytolacea americana* II; (6) *Spirulina platensis*.

Table 1. *Statistics of observed structure factors of the native crystal*

d^{-2} (Å^{-2})	0.00–0.06	–0.12	–0.18	–0.24	–0.31	Total
N*	1314	2364	2990	3600	4670	14938
$N1$*	1286	2275	2798	3200	4006	13565
$N3$*	1130	1959	2287	2626	2849	10851
Completeness†	0.98	0.96	0.94	0.89	0.86	0.91

*N, $N1$ and $N3$ are the theoretical number of unique refections, the numbers of observed reflections of the native crystal with F values greater than $1\sigma_F$ and $3\sigma_F$, respectively.

† Completeness is evaluated by the formula, $N1/N$.

respectively, and the R factor for the reflections between 6 and 3 Å resolution was calculated at each translational position. The minimum R value was 0.353 at the translational position of (dx, dy, dz) = (0.010, -0.003, 0.002) in fractional coordinates. Assuming the molecules were rigid bodies, we refined six positional and six rotational parameters for two independent molecules in the asymmetric unit with reflections between 5 and 2.5 Å resolution by *CORELS* (Sussman, 1985). After the several cycles of the refinement, all the translational and the rotational parameters converged well and the R value was reduced from 0.405 to 0.376. The structure was refined at 2.5 Å resolution by restrained least-squares refinement (Hendrickson & Konnert, 1980). After 45 cycles of the refinement the R value was reduced to 27.2%. Although further refinement was continued at 2.2 Å resolution, it was time-consuming to remove false minima by manual revision. Thus, we switched from the restrained least-squares method to a simulated-annealing (SA) method with the program *X-PLOR* (Brünger, 1988). The SA refinement procedure is given in Table 2. The first to the fourth steps of the refinement consisted of heating and cooling stages. Further repetitions of the refinement were carried out by slow cooling. Abnormal structures were corrected by using *FRODO* in a $(2F_o - F_c)$ omit map calculated according to Bhat (1988) after each repetition from the first to sixth refinement. Water molecules were picked up in a $(2F_o - F_c)$ map or a $(F_o - F_c)$ map. The structures of protein molecules as well as those of water molecules were refined by the restrained least-squares refinement at 1.8 Å resolution.

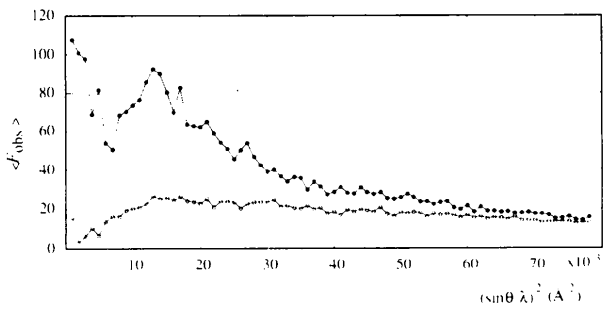

Fig. 2. The average observed structure amplitudes for $h + k = 2n$ (closed circle) and $h + k = 2n + 1$ (open circle) in each resolution shell.

Non-crystallographic symmetry restraints between the two molecules in the asymmetric unit were released during the SA refinements at 2.2 and 1.8 Å resolution and the restrained refinement at 1.8 Å resolution. Solvent sites and protein structures were manually revised every 15 to 30 cycles of the refinement in the $(F_o - F_c)$ and $(2F_o - F_c)$ maps. The occupancies of all atoms were fixed at 1.0. Positional and individual thermal parameters for 1420 non-H protein atoms and 183 water molecules were refined at the final stage of the refinement. Several cycles of the final refinement were carried out without structural restraints for [2Fe-2S] centers. After 430 cycles of the refinement the R factor was reduced to 0.170 for 13 838 reflections ($F > 1\sigma_F$) in the resolution range 10.0–1.8 Å. The final weights for the restraints and the final deviations from idealities are listed in Table 3. The distribution of the R factors as a function of $2\sin\theta/\lambda$ (Fig. 3) indicates that the estimated r.m.s. error of the atomic positions (Luzzati, 1952) is about 0.2 Å. The coordinates and individual temperature factors of the present molecules have been deposited in the Protein Data Bank (Bernstein *et al.*, 1977).*

Results and discussion

General structure

Most parts of the final structure for each molecule fit well to the $(2F_o - F_c)$ map except the N-terminal and three C-terminal residues. The following atoms were located in lower electron-density regions than the others. For molecule *A*: Cα, Cβ, C and O of Ala1; Nζ of Lys3; Cβ of Leu15; Cδ of Pro18; Cδ and Oε1 of Glu29; Cβ of Ala40; Cα of Ser58; Oε1 and Oε2 of Glu59; Cγ, Cδ, Oε1 and Oε2 of Glu69; Cβ, Cγ, Cδ, Oε1, Oε2 and O of Glu93; Cδ1 and Cδ2 of Leu94; Cα, Cβ, C, O and a terminal O atom of Phe95. For molecule *B*: Cα and C of Ala1; Nζ of Lys3; Cε and Nζ of Lys7; Oγ of Ser10; Cδ, Oε1 and Oε2 of Glu29; Oε1 and Oε2 of Glu59; Cβ of Ser61; Cγ, Cδ, Oε1 and Oε2 of Glu69; N, Cγ, Cδ, Oε1 and Oε2 of Glu92; N, Cβ, Cγ, Cδ, Oε1 and Oε2 of Glu93; Cγ, Cδ1, Cδ2 and O of Leu94; N, Cα and a terminal O atom of Phe95.

The main-chain fold and the active center of molecule *A* are shown in Fig. 4. β-sheets are formed by the residues Tyr2-Thr8, Gly11-Val7, Lys49-Val51 and Asp83-Glu87 at the bottom of the standard view, and α-helices by residues Ile23-Ala30, Asp65-Glu70 and Glu91-Phe95. Only one α-helix had been assigned in each molecule of *A. sacrum* and *S. platensis* Fd's, which corresponds to the α-helix of Ile23-Ala30 of the *E.*

* Atomic coordinates and structure factors have been deposited with the Protein Data Bank, Brookhaven National Laboratory (Reference: 1FRR, R1FRRSF). Free copies may be obtained through The Technical Editor, International Union of Crystallography, 5 Abbey Square, Chester CH1 2HU, England (Supplementary Publication No. SUP 37102). A list of deposited data is given at the end of this issue.

Table 2. *Summary of SA refinement*

	1		2		3		4		5	6	7
Stage	Heat	Cool	Heat	Cool	Heat	Cool	Heat	Cool	Slow cool	Slow cool	Slow cool
Temperature (K)	2000	300	2000	300	6000	300	6000	300	4000 to 300	6000 to 300	6000 to 300
No. of steps	1000	250	1000	250	5000	500	4000	500			
Cooling rate (fs K^{-1})									25/25	25/25	25/25
Resolution (Å)	6.0–2.2		6.0–2.2		6.0–2.2		6.0–2.2		6.0–2.0	6.0–1.8	6.0–1.8
No. of reflections*	6364		6364		6364		6364		8416	10181	10181
R (initial)	0.322		0.280		0.270		0.264		0.276	0.257	0.293
R (final)	0.280		0.263		0.269		0.253		0.247	0.242	0.216

* The reflections with $F > 3\sigma_F$ are included in the refinement. Time steps during stages 1–4 were 1.0 fs, and those for slow-cooling 0.5 fs. The temperature factor for each atom was kept at 14.2 $Å^2$ during stages 1–4 and individual temperature factors were refined during stages 5–7. A total of 1420 atomic positions were refined in the procedures.

Table 3. *Statistics at the final cycle in the restrained least-squares refinement*

	Target σ	R.m.s. deviation	No. of parameters
Bond length (1–2 neighbors) (Å)	0.020	0.014	1434
Angles corresponding to (1–3 neighbors) (Å)	0.040	0.042	1944
Planes corresponding to (1–4 neighbors) (Å)	0.050	0.046	474
Planar groups (Å)	0.020	0.012	1246
Chiral volumes ($Å^3$)	0.150	0.150	226
van der Waals contacts			
Single-torsion contacts (Å)	0.500	0.191	492
Multiple-torsion contacts (Å)	0.500	0.282	389
Possible hydrogen-bonding contacts (Å)	0.500	0.220	131
Torsion angles			
Peptide plane (Å, °)	3.0	2.1	190
Staggered torsion contacts (60/120°)	15.0	19.0	238
Orthonormal torsion contacts (90°)	20.0	19.4	16
Isotropic temperature factors			
Main-chain (1–2 neighbors) ($Å^2$)	2.0	3.61	790
Main-chain (1–3 neighbors) ($Å^2$)	2.0	4.72	1000
Side-chain (1–2 neighbors) ($Å^2$)	3.0	6.61	644
Side-chain (1–3 neighbors) ($Å^2$)	3.0	8.95	944

arvense Fd. The helix of Asp65-Glu70 for the present Fd was located clearly in the electron-density distribution as the residues between 67 and 73 of anabaena 7120 Fd (Rypniewski *et al.*, 1991). A probable reason why the helical structure corresponding to the helix of Asp65-Glu70 of *E. arvense* was not detected in *A. sacrum* and *S. platensis* Fd's is that the corresponding regions of these algal Fd's were poor in electron-density distribution. Several residues at the C terminus were located in low electron-density regions and/or have high temperature factors for all [2Fe-2S] Fd's so far investigated crystallographically. There may be high flexibility in this region for the [2Fe-2S] Fd's.

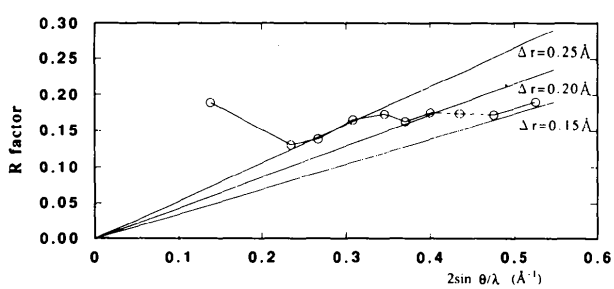

Fig. 3. The distribution of R factors as a function of $2\sin\theta/\lambda$.

The Ramachandran plot of molecules *A* and *B* is shown in Fig. 5, which indicates that α-helical and β-structural conformations are prominent. Six out of nine glycine residues of the molecules are outside the 'extreme limiting contact region' given for polyalanine by Ramakrishnan & Ramachandran (1965).

Structure of the [2Fe-2S] *active center*

Bond distances and angles of [2Fe-2S] active centers for the two independent molecules together with their average values are listed in Table 4. The structures of the active centers of the two molecules in an asymmetric unit are identical to each other within experimental errors. The polypeptide loop around the [2Fe-2S] center is shown in Fig. 6. The two Fe atoms are coordinated tetrahedrally by two inorganic S atoms and two cysteinyl S atoms like those found in other [2Fe-2S] Fd's. One Fe atom is coordinated by the Sγ atoms of Cys38 and Cys43 and the other by those of Cys46 and Cys76.

An Fe—Fe distance of 2.76 Å indicates a metal-metal interaction and a distance between two inorganic S atoms (S*) of 3.49 Å is too long for any significant bonding between the atoms as in the synthetic analogs (Mayerle, Denmark, DePamphilis, Ibers & Holm, 1975). Fig. 7 shows torsion about the Fe—Sγ bonds in which Sγ—Cβ angles are about 60° for three cases and 30° for one case. This is consistent with the statistics of the torsion angles for the [4Fe-4S] cluster in several iron-sulfur proteins (Bernstein *et al.*, 1977; Adman, Sieker, & Jensen, 1976; Carter, Kraut, Freer & Alden, 1974), in which 31 out of 57 torsion angles are within the angle range 60 (15)°. NH···S and OγH···S hydrogen bonds around the [2Fe-2S] cluster given in Table 5 stabilize the loop structure around the active center. Most of the hydrogen bonds are conserved among the known plant and algal [2Fe-2S] Fd's.

Intermolecular interaction and molecular packing

A stereoview of the molecular packing is shown in Fig. 8. Eight types of intermolecular interaction (Table 6 and Fig. 9) were assigned. Interactions I, IV and V are related by pseudo (*a* + *b*)/2-translational symmetries to I′, IV′ and V′, respectively. Interactions II and III have pseudo-twofold symmetries within themselves.

Structural comparison between molecules A and B

The displacement of each residue is given in Fig. 10. The root-mean-square (r.m.s.) deviation of equivalent Cα atoms of two independent molecules superposed by a least-squares program *SUPPOS* (Nishikawa & Ooi, 1980) was 0.26 Å. The displacements of corresponding Cα atoms of two molecules are larger than 0.3 Å for the residues of Ala1, Val17-Glu19, Gly53-Ser54, Gly60-Ser61, Gln67, Glu69-Glu70, Ser82 and Glu92-Phe95. The residues Ala1 and Glu92-Phe95 of both

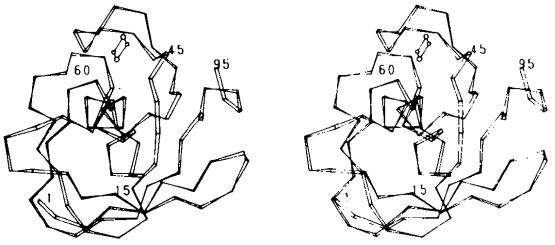

Fig. 4. Stereoscopic ribbon drawing of the *E. arvense* Fd with Cα backbone and [2Fe-2S] cluster atoms. This stereo picture will be used as the standard view of [2Fe-2S] Fd's in the text.

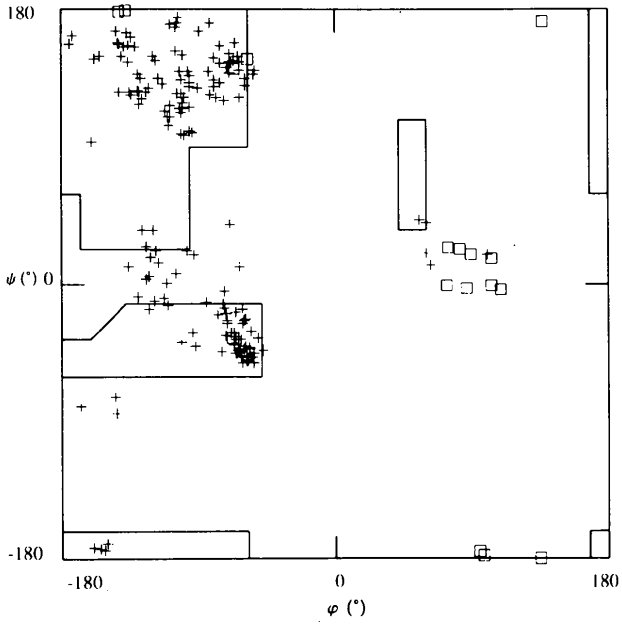

Fig. 5. Ramachandran plot of the main-chain dihedral angles of molecules *A* and *B*. Glycine residues are shown as squares.

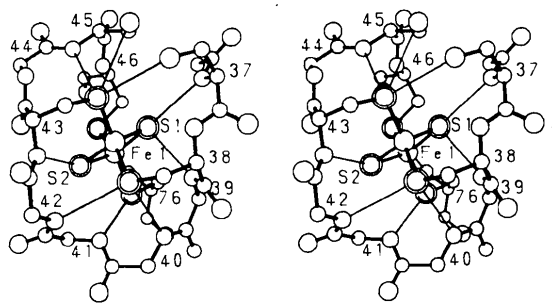

Fig. 6. The polypeptide chain around the active center. S, O and N atoms are illustrated by large double circles, a large circle and a medium open circle, respectively. Hydrogen bonds are illustrated by thin lines. Hydrogen bonds were assigned by the interatomic distances and angles given in Table 4.

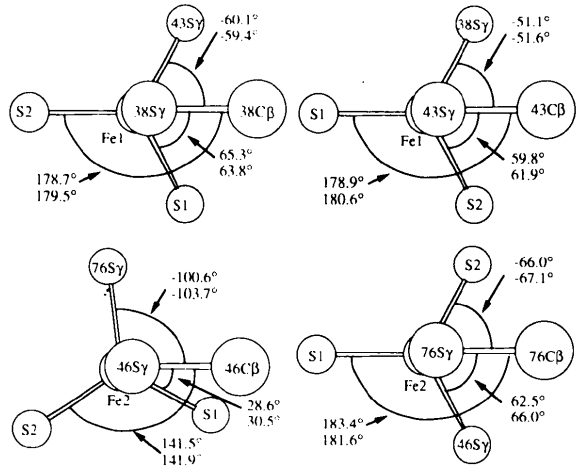

Fig. 7. Projection along Sγ—Fe bonds. Torsion angles were measured clockwise from a Sγ—Cβ bond. Upper values are those for molecule *A* and lower ones for molecule *B*.

Table 4. *Distances, angles and their average values with e.s.d.'s for* [2Fe–2S] *clusters*

Distances (Å)	Molecule *A*	Molecule *B*
38Sγ—Fe1	2.23	2.31
43Sγ—Fe1	2.22	2.24
46Sγ—Fe2	2.26	2.25
76Sγ—Fe2	2.23	2.24
Mean Sγ—Fe	2.24 (3)	
Fe1—S1	2.17	2.11
Fe1—S2	2.33	2.24
Fe2—S1	2.29	2.27
Fe2—S2	2.25	2.30
Mean Fe—S	2.26 (7)	
Fe1—Fe2	2.81	2.75
Mean Fe1—Fe2	2.78 (3)	
S1—S2	3.54	3.51
Mean S1—S2	3.53 (2)	
38Sγ—38Cβ	1.88	1.84
43Sγ—43Cβ	1.82	1.86
46Sγ—46Cβ	1.86	1.84
76Sγ—76Cβ	1.78	1.85
Mean Sγ—Cβ	1.84 (3)	

Angles (°)	Molecule *A*	Molecule *B*
S1—Fe1—S2	103.7	107.2
S1—Fe2—S2	102.3	100.2
Mean S—Fe—S	103 (3)	
38Sγ—Fe1—S1	121.3	118.2
38Sγ—Fe1—S2	99.3	101.0
43Sγ—Fe1—S1	108.7	109.5
43Sγ—Fe1—S2	114.9	115.1
46Sγ—Fe2—S1	114.8	117.8
46Sγ—Fe2—S2	106.6	104.0
76Sγ—Fe2—S1	113.3	114.0
76Sγ—Fe2—S2	110.2	107.9
Mean Sγ—Fe—S	111 (6)	

Angles (°)	Molecule *A*	Molecule *B*
Fe1—S1—Fe2	78.0	77.6
Fe1—S2—Fe2	75.7	76.7
Mean Fe—S—Fe	77 (1)	
Fe1—38Sγ—38Cβ	120.6	120.9
Fe1—43Sγ—43Cβ	114.1	123.5
Fe2—46Sγ—46Cβ	107.0	107.8
Fe2—76Sγ—76Cβ	105.7	101.8
Mean Fe—Sγ—Cβ	113 (8)	
38Sγ—Fe1—43Sγ	108.9	106.0
46Sγ—Fe2—76Sγ	109.3	111.3
Mean Sγ—Fe—Sγ	109 (2)	

Table 5. *Hydrogen bonds around the* [2Fe—2S] *active centers of molecules A and B*

Numbers before atomic symbols are the sequence numbers.

Distances (Å)	Molecule *A*	Molecule *B*
S1—37N	3.24	3.30
38Sγ—40N	3.32	3.30
38Sγ—42N	3.41	3.43
43Sγ—37Oγ	3.27	3.12
43Sγ—45Oγ	3.49	3.52
43Sγ—45N	3.20	3.28
76Sγ—41N	3.64	3.63

Angles (°)	Molecule *A*	Molecule *B*
37N—S1—Fe1	115.5	117.2
40N—38Sγ—38Cβ	97.5	100.3
42N—38Sγ—38Cβ	138.6	140.0
37Oγ—43Sγ—43Cβ	117.2	118.4
45Oγ—43Sγ—43Cβ	123.5	111.5
45N—43Sγ—43Cβ	109.9	101.2
41N—76Sγ—76Cβ	154.4	154.0

Angles (°)	Molecule *A*	Molecule *B*
40N—38Sγ—Fe1	105.9	105.7
42N—38Sγ—Fe1	95.4	92.1
37Oγ—43Sγ—Fe1	104.2	104.3
45Oγ—43Sγ—Fe1	122.3	124.9
45N—43Sγ—Fe1	109.9	111.7
41N—76Sγ—Fe2	91.5	93.0

Table 6. *Intermolecular contacts*

Intermolecular interactions with close contacts shorter than 4.0 Å are listed in this table. Definitions of molecular names are given in Fig. 9.

Scheme	Molecule 1	Residues	Molecule 2	Residues
I	*A*1	1Ala, 16Asp, 18Pro, 26Ala, 29Glu, 30Ala	*B*1	94Leu, 95Phe
I′	*B*1	1Ala, 18Pro, 19Glu, 26Ala, 29Glu	*A*8	64Asp, 67Gln, 94Leu, 95Phe
II	*A*1	52Ser, 53Gly, 54Ser, 69Glu, 81Glu, 82Ser, 83Asp	*B*6	52Ser, 53Gly, 54Ser, 69Glu, 81Glu, 82Ser, 83Asp
III	*A*1	28Glu, 33Asp, 34Leu, 35Pro, 36Phe, 37Ser, 38Cys, 45Ser, 91Glu	*B*3	28Glu, 33Asp, 34Leu, 35Pro, 36Phe, 37Ser, 38Cys, 45Ser, 91Glu, 92Glu
IV	*A*1	19Glu, 20Gly	*A*7	9Pro, 11Gly
IV′	*B*1	19Glu, 20Gly	*B*7	10Ser, 11Gly
V	*A*1	11Gly, 12Glu, 13Phe, 14Thr	*B*7	19Glu, 20Gly, 62Phe, 63Leu, 64Asp, 65Asp
V′	*B*1	11Gly, 12Glu, 13Phe, 14Thr, 30Ala, 32Tyr	*A*4	61Ser, 63Leu, 64Asp, 65Asp

molecules are located in poor electron-density regions and the temperature factors for these residues are very high (Fig. 12). This indicates that the residues are flexible even in the crystal.

There may be several factors which cause distortion of the molecules. Gly53 residues of molecules *A* and *B* are in close contact with each other at a pseudo-twofold axis (Fig. 11*a*). The close contact causes structural differences between the two Gly53 residues of molecules *A* and *B* by 0.38 Å at the Cα position. Except for both polypeptide termini the two molecules exhibit the largest structural difference of 0.6 Å at Cα of Glu19 (Fig. 11*b*). The side-chain atoms, Cδ and Oε1, of Glu19 of molecule *A* interact with atoms of another molecule in the interaction scheme IV. On the other hand, Cβ, Cγ, Cδ, and Oε1 of Glu19 of molecule *B* contact closely with other molecules in the schemes I′, IV′ and V. These different interaction schemes result in the large structural difference between two molecules around Glu19.

A superposition of the segment Gly60-Ser61-Phe62 of molecules *A* and *B* is shown in Fig. 11(*c*). The displacements for 61O and 61Cα are 0.9 and 0.5 Å, respectively. This might be caused by a hydrogen bond between a water molecule and Oγ of Ser61 of molecule *A*. The similar perturbation by a hydrogen bond between a water molecule and a carbonyl O atom is found for Pro9, where a carbonyl O atom at Pro9 of molecule *A* is as far as 0.5 Å from that of molecule *B*.

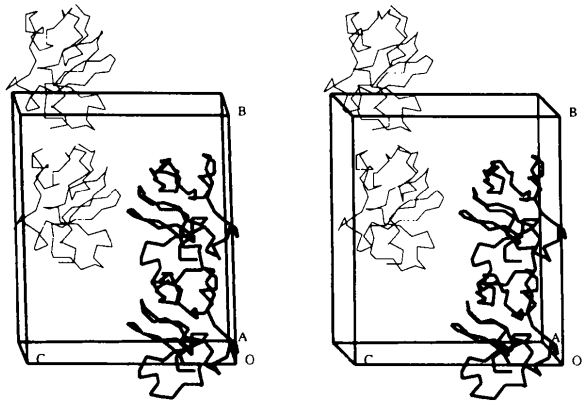

Fig. 8. Molecular packing in the crystal drawn by a stereo pair projected along *a* axis. An asymmetric unit contains two molecules drawn by heavy lines. The molecules represented by thin lines are related to those represented by heavy lines by a 2_1 symmetry.

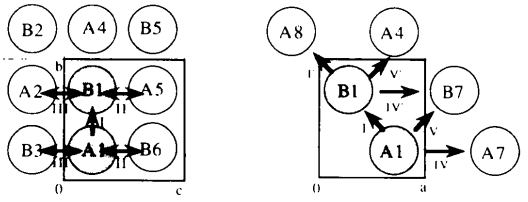

(*a*) (*b*)

Fig. 9. Schematic drawings of intermolecular interactions illustrated with projections on (*a*) the *bc* plane and (*b*) the *ab* plane. Letters *A* and *B* represent molecules *A* and *B*, respectively. Numerals following the letters indicate symmetry operations: 1 = *x*, *y*, *z*; 2 = -*x*, 1/2 + *y*, -*z*; 3 = -*x*, -1/2 + *y*, -*z*; 4 = *x*, 1 + *y*, *z*; 5 = -*x*, 1/2 + *y*, 1 - *z*; 6 = -*x*, -1/2 + *y*, 1 - *z*; 7 = -1 + *x*, *y*, *z*; 8 = -1 + *x*, 1 + *y*, *z*.

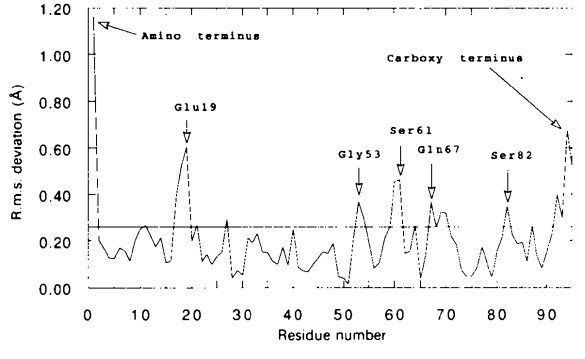

Fig. 10. The r.m.s. deviation of equivalent Cα-atom positions between molecules *A* and *B*. The two molecules were superposed by the least-squares method. The average deviation of 0.26 Å is shown by a horizontal line. The maximum deviation is 0.60 Å of Glu19 except for both termini.

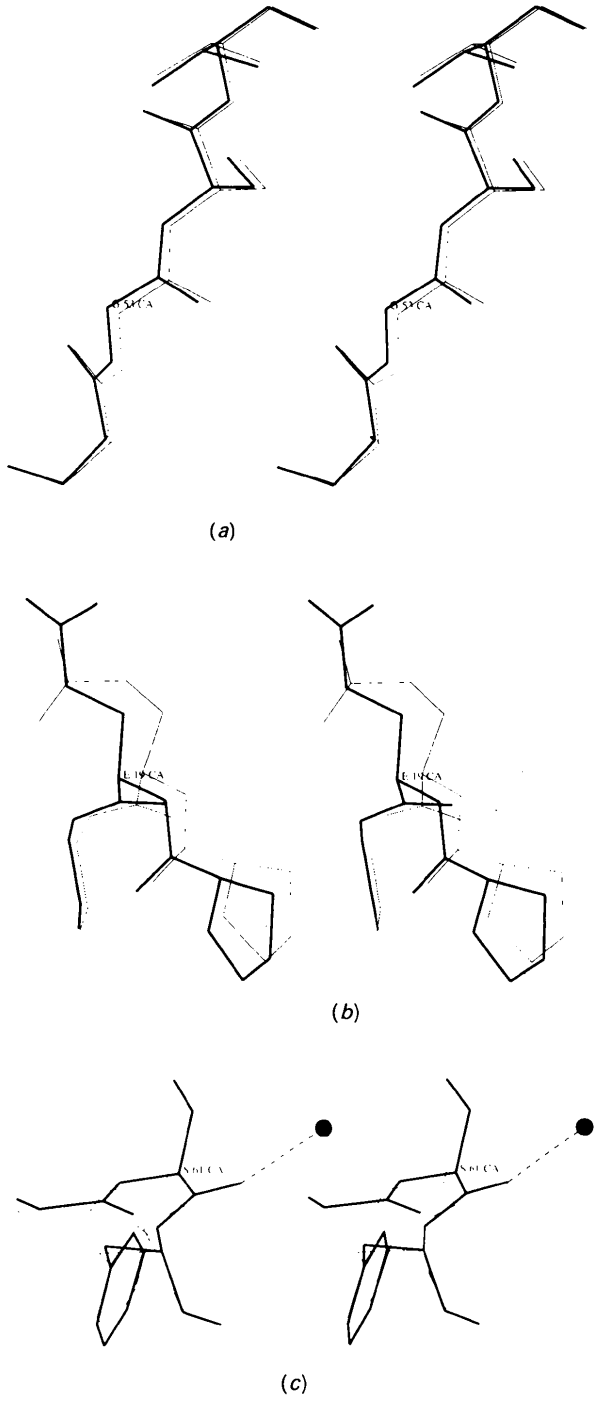

(*a*) (*b*) (*c*)

Fig. 11. Superposition of molecule *A* (heavy lines) and molecule *B* (thin lines). Closed circles represent water. (*a*) Segment of Ser52-Gly53-Ser54-Val55. The Cα atoms of the two glycine residues deviate by 0.38 Å. These residues contact closely with each other at a pseudo-twofold axis in the interaction scheme II. (*b*) Segment of Pro18-Glu19-Gly20. The deviation between two Cα atoms of Glu19 is 0.60 Å. The side chains of Glu19 for both molecules take quite different conformations. (*c*) Segment of Gly60-Ser61-Phe62. Molecule *A* has a hydrogen bond between O of Ser61 and a water molecule, while molecule *B* has no such hydrogen bond. Carbonyl O and Cα atoms of Ser61 are shifted toward the water molecule in molecule *A*.

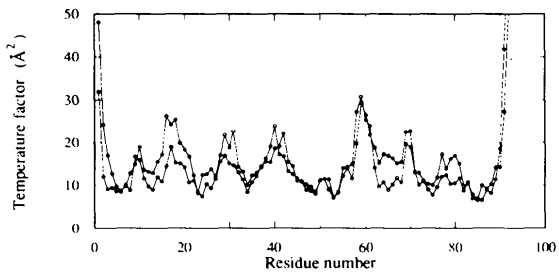

Fig. 12. Temperature factors of the residues for molecules *A* (open circles) and *B* (closed circles). Each value was estimated by averaging over the temperature factors of the main-chain atoms in a given residue.

Fig. 12 shows temperature factors of main-chain atoms for molecules *A* and *B*. It is obvious that the temperature factors of the two molecules are highly correlated. They have a correlation coefficient of 0.98, which is defined by the formula,

$$\Sigma(B_{Ai} - B_A)(B_{Bi} - B_B)/[\Sigma(B_{Ai} - B_A)^2(B_{Bi} - B_B)^2]^{1/2},$$

where B_{Ai} and B_{Bi} are temperature factors of ith residues of molecules *A* and *B*, and B_A and B_B are the average temperature factors of molecules *A* and *B*, respectively. Thus, both molecules preserve a common elastic feature in the crystalline state. The residues with large structural differences between the two molecules have high temperature factors.

We are grateful to Mr Sigeo Sawada for his help in preparation and crystallization of the protein and to Mr Kazuhiko Takahashi for his help in intensity data processing. This work was supported in part by a Grant-in-Aid for Special Project Research (No. 62220023) from the Ministry of Education, Science and Culture of Japan.

References

ADMAN, E. T., SIEKER, L. C. & JENSEN, L. H. (1976). *J. Biol. Chem.* **251**, 3801-3806.

BERNSTEIN, F. C., KOETZLE, T. F., WILLIAMS, G. J. B., MAYER, E., BRICE, M. D., RODGERS, J. R., KENNARD, O., SHIMANOUCHI, T. & TASUMI, M. (1977). *J. Mol. Biol.* **112**, 535-542

BHAT, T. N. (1988). *J. Appl. Cryst.* **21**, 279-281.

BRÜNGER, A. T. (1988). *J. Mol. Biol.* **203**, 803-816.

CARTER, C. W. JR, KRAUT, J., FREER, S. T. & ALDEN, R. A. (1974). *J. Biol. Chem.* **249**, 6339-6346.

DUGAD, L. B., LAMAR, G. N., BANCI, L. & BERTINI, I. (1990). *Biochemistry*, **29**, 2263-2271.

FUKUYAMA, K., HASE, T., MATSUMOTO, S., TSUKIHARA, T., KATSUBE, Y., TANAKA, N., KAKUDO, M., WADA, K. & MATSUBARA, H. (1980). *Nature (London)*, **286**, 522-524.

GRONENBORN, A. M., FILPULA, D. R., ESSIG, N. Z., ACHARI, A., WHITLOW, M., WINGFIELD, P. T. & CLORE, G. M. (1991). *Science*, **253**, 657-661.

HASE, T., WADA, K. & MATSUBARA, H. (1977). *J. Biochem.* **82**, 277-286.

HENDRICKSON, W. A. & KONNERT, J. H. (1980). *Computing in Crystallography*, edited by R. DIAMOND, S. RAMESESHAN & K. VENKATESAN, pp. 13.01-13.25. Bangalore: Indian Academy of Sciences.

LOVENBERG, W. (1973, 1977). Editor. *Iron-Sulfur Proteins*, Vol. I-III. London, New York: Academic Press.

LUZZATI, V. (1952). *Acta Cryst.* **5**, 802-810.

MATSUBARA, H. & HASE, T. (1983). *Proteins and Nucleic Acids in Plant Systematics*, edited by U. JENSEN & D. E. FAIRBROTHERS, pp. 168-181. Berlin: Springer-Verlag.

MATSUBARA, H. & SAEKI, K. (1992). *Adv. Inorg. Chem.* **38**, 223-280.

MATTHEWS, B. W. (1968). *J. Mol. Biol.* **33**, 491-497.

MAYERLE, J. J., DENMARK, S. E., DEPAMPHILIS, B. V., IBERS, J. A. & HOLM, R. H. (1975). *J. Am. Chem. Soc.* **97**, 1032-1045.

MINO, Y., LOEHR, T. M., WADA, K., MATSUBARA, H. & SANDERS-LOEHR, J. (1987). *Biochemistry*, **26**, 8059-8065.

NISHIKAWA, K. & OOI, T. (1980). *Program System for Protein Conformation Study*, pp. 45-49.

NORTH, A. C. T., PHILLIPS, D. C. & MATTHEWS, F. S. (1968). *Acta Cryst.* A**24**, 351-359.

OH, B. H. & MARKLEY, J. L. (1990). *Biochemistry*, **29**, 3993-4004.

RAMAKRISHNAN, C. & RAMACHANDRAN, G. N. (1965). *Biophys. J.* **5**, 909-933.

RYPNIEWSKI, W. R., BREITER, D. R., BENNING, M. M., WEISSENBERG, G., OH, B., MARKLEY, J. L., RAYMENT, I. & HOLDEN, H. M. (1991). *Biochemistry*, **30**, 4126-4131.

SUSSMAN, J. L. (1985). *Methods Enzymol.* **115**, 271-303.

TSUKIHARA, T., FUKUYAMA, K., MIZUSHIMA, M., HARIOKA, T., KUSUNOKI, M., KATSUBE, Y., HASE, T. & MASTUBARA, H. (1990). *J. Mol. Biol.* **216**, 399-410.

TSUKIHARA, T., FUKUYAMA, K., NAKAMURA, M., KATSUBE, Y., TANAKA, N., KAKUDO, M., HASE, T., WADA, K. & MATSUBARA, H. (1981). *J. Biochem.* **90**, 1763-1773.

VIJAY-KUMAR, S., BUGG, C. E. & COOK, W. J. (1987). *J. Mol. Biol.* **194**, 531-544.